Contribution from the Department of Chemistry,
William Marsh Rice University, Houston, Texas 77001

Bis(*N*-methylethylenediaminesalicylaldiminato)iron(III) Complexes. Magnetic, Mössbauer, and Intersystem Crossing Rate Studies in the Solid and Solution States for a New ($S = {}^1/_2$) $\rightleftarrows$ ($S = {}^5/_2$) Spin-Equilibrium Case[1]

RANDALL H. PETTY,[2] ERIC V. DOSE,[3,4] MICHAEL F. TWEEDLE,[4] and LON J. WILSON*

Received July 21, 1977

Bis(*N*-methylethylenediaminesalicylaldiminato)iron(III) complexes, [Fe(X-Salmeen)$_2$](PF_6), with their FeN_4O_2 cores have been shown by variable-temperature magnetic susceptibility (10–300 K) and Mössbauer spectroscopy to be new (low-spin, $S = {}^1/_2$) $\rightleftarrows$ (high-spin, $S = {}^5/_2$) spin-equilibrium compounds in the solid state. From the Mössbauer spectra, an *upper* limit of $\sim 10^7$ s^{-1} has been established for the rate of

$$(S = {}^1/_2) \underset{k_{-1}}{\overset{k_1}{\rightleftarrows}} (S = {}^5/_2)$$

intersystem crossing in the solid state. The spin equilibria are also supported in the solution state, as verified by variable-temperature (200–300 K) magnetic susceptibility and electronic spectroscopy measurements. In solution, laser Raman temperature-jump kinetics has been employed to directly measure the forward (k_1) and reverse (k_{-1}) rate constants for the intersystem crossings with 2×10^7 $s^{-1} \lesssim k \lesssim 2 \times 10^8$ s^{-1}. Intersystem crossing rate constant data for these bis-tridentate [Fe^{III}(X-Salmeen)$_2$]$^+$ complexes are discussed and compared to data already available for the electronically similar (same FeN_4O_2 core) but structurally different (hexadentate ligand) spin-equilibrium species, [Fe^{III}(Sal)$_2$trien]$^+$.

Introduction

Our recent studies of spin-equilibrium phenomena for six-coordinate iron(III),[5-7a] iron(II),[8-10] and cobalt(II)[11] complexes have focused on the solution state where forward (k_1) and reverse (k_{-1}) rate constants for *dynamic*

$$\text{(low spin, ls)} \underset{k_{-1}}{\overset{k_1}{\rightleftarrows}} \text{(high spin, hs)}$$

spin-interconversion (intersystem crossing) have been found measurable by laser Raman temperature-jump[12,13] and ultrasonic relaxation[14] kinetics. To date, measured rate constants in solution for synthetically derived spin–equilibrium compounds have been found to range from 4×10^5 to 2×10^7 s^{-1}, with the corresponding range for the spin state lifetime (τ(spin state) = k^{-1}) being 50–2500 ns. Most recently, the first such measurement of intersystem crossing in a metalloprotein, metmyoglobin hydroxide, has yielded forward and reverse rate constants of 3.9×10^7 and 2.8×10^7 s^{-1}, respectively.[15]

The impetus for these studies has been threefold: (1) to better understand radiationless intersystem crossing phenomena as they pertain to photochemically induced excited states, (2) to assess the effect of spin multiplicity changes on electron-transfer rates, and (3) to determine the fundamental electronic and/or molecular structural factors which are rate determining for intersystem crossing processes in electronically unusual spin-equilibrium metal complexes. The latter consideration is the primary focus of this work which reports the synthesis, characterization, and study of the low-spin (^{2}T, $S = {}^1/_2$) $\rightleftarrows$ high-spin (^{6}A, $S = {}^5/_2$) phenomena associated with a new family of spin-equilibrium iron(III) compounds, the bis(*N*-methylethylenediaminesalicylaldiminato)iron(III) complexes ([Fe(X-Salmeen)$_2$]$^+$), shown in Figure 1A. These particular compounds, with their FeN_4O_2 core, have been singled out for study since they are electronically similar to the already investigated [Fe(X-Sal)$_2$trien]$^+$ species of Figure 1B,[5] yet the former have bis-tridentate structures while a recent x-ray structural analysis[16] has verified the hexadentate structure of the latter. Thus, by critically comparing the spin-equilibrium properties of the two systems, it was hoped that the influence, if any, of their differing molecular structure on the intersystem crossing kinetics could be directly observed.

Experimental Section

Physical Measurements. Variable-temperature magnetic susceptibilities in the solid state were measured by the Faraday technique using equipment and procedures previously described.[7] Pascals' constants were used to correct for ligand and anion diamagnetism: for X-Salmeen, -177.5×10^{-6} cgsu for X = H, -212.9×10^{-6} cgsu for X = OCH_3, -198.1×10^{-6} cgsu for X = NO_2; PF_6^-, -64.1×10^{-6} cgsu; H_2O, -13×10^{-6} cgsu. Magnetic measurements in solution were performed by the Evans ^{1}H NMR method[17] with methanol being used for temperature calibration. The measurements were corrected for changes in solvent density and sample concentration with temperature.[18] Chloroform was used as the reference compound.

Solid- and solution-state infrared spectra were obtained on a Beckman IR-20 using NaCl plates and Nujol mulls for the solids and Beckman IR-Tran 2 cells for the solutions. Solution conductivities were measured using a Model 31 YS1 conductivity bridge. UV–vis spectra were obtained on a Cary 17 recording spectrophotometer using jacketed, insulated quartz cells; sample temperatures were monitored using a thermistor and are ±0.5 °C.

Mössbauer spectra of the solids were obtained using a previously described spectrometer[5] and computer analyzed by the program of Chrisman and Tumolillo.[19] The temperature was measured with a copper–constantan thermocouple imbedded in the sample. Computer-generated plots of the Mössbauer spectra were obtained using a Calcomp program written by E. V. Dose.

The temperature-jump experiments were performed using the laser-stimulated Raman apparatus previously described.[12] For the experiments sample cells with 0.020–0.081 mm path lengths were employed. A 1:5 acetone–methanol solvent mixture was used, and relaxation data were obtained in thermostated cells (±2 °C), by monitoring band maxima of the high-spin or low-spin electronic absorption bands in the visible region; in all cases, [Fe] $\approx 10^{-3}$ M. The relaxation traces which were obtained from photographs of oscilloscope traces measured the change in optical density of the sample spectrum with time (ns). The method and data treatment are described in the text.

Materials and Syntheses. *N*-Methylethylenediamine (98%) and the X-salicylaldehydes were obtained from Aldlrich and used without further purification. Spectroquality acetone, CH_3OH, $CHCl_3$, and CH_2Cl_2 were used for the ^{1}H NMR and IR studies without further purification. Chemical analyses were obtained commercially.

[Fe(Salmeen)$_2$](PF_6) was prepared by adding *N*-methylethylenediamine (1.6 g, 20 mmol) in 20 mL of methanol to a solution of

0020-1669/78/1317-1064$01.00/0

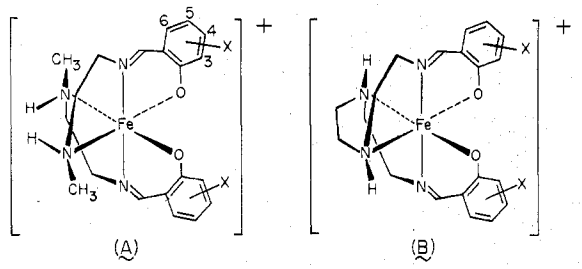

Figure 1. (A) The bis-tridentate structure of the $[Fe(X\text{-Salmeen})_2]^+$ cations. (B) The hexadentate structure of the $[Fe(X\text{-Sal})_2trien]^+$ cations.

salicylaldehyde (2.44 g, 20 mmol) in 20 mL of methanol. The solution immediately turned dark yellow and was allowed to stir 5 min. To this stirring solution, $NaOCH_3$ (1.08 g, 20 mmol) dissolved in 50 mL of methanol was added and the solution stirred an additional 15 min. To the solution $Fe(NO_3)_3 \cdot 9H_2O$ (4.04 g, 10 mmol) dissolved in 15 mL of methanol was then slowly added, producing a color change to dark purple. After 10 min, the solution was filtered and KPF_6 (3.8 g, 20 mmol) dissolved in methanol was added with filtration. The solution was reduced in volume under vacuum until precipitation occurred. The solid was recrystallized twice from a CH_2Cl_2/CCl_4 solution, and the resulting red-purple crystals were washed with methanol and then ether and dried in vacuo at 117 °C over P_2O_5 for 12 h. Yield 2.75 g, 45%. The compound is thermochromic in solution changing, for example, from purple at room temperature to blue by −80 °C in acetone. Anal. Calcd: C, 43.26; H, 4.72; N, 10.09. Found: C, 43.03; H, 4.40; N, 9.99. Λ_c = 163.1 μmho cm^{-1} at 30 °C and 10^{-3} M in acetone.

[Fe(3-OCH$_3$Salmeen)$_2$](PF$_6$) was prepared as described above for the parent compound except that 3.04 g (20 mmol) of 3-methoxysalicylaldehyde was used. The product was isolated as a green powder. Yield 1.35 g, 22%. The compound is thermochromic in solution, changing from dark purple at room temperature to blue by −80 °C in acetone. Anal. Calcd: C, 42.94; H, 4.91; N, 9.11. Found: C, 43.07; H, 4.75; N, 8.77. Λ_c = 153 μmho cm^{-1} at 30 °C and 10^{-3} M in acetone.

[Fe(4-OCH$_3$Salmeen)$_2$](PF$_6$) was prepared as above for the parent compound except that 3.04 g (20 mmol) of 4-methoxysalicylaldehyde was used. The product was isolated as dark purple crystals. Yield 1.46 g, 23%. The compound is thermochromic in solution, changing from red at room temperature to purple by −80 °C in acetone. Anal. Calcd: C, 42.94; H, 4.91; N, 9.11. Found C, 42.82; H, 4.90; N, 9.27. Λ_c = 132 μmho cm^{-1} at 30 °C and 10^{-3} M in acetone.

[Fe(5-OCH$_3$Salmeen)$_2$](PF$_6$) was prepared as above for the parent compound except 3.04 g (20 mmol) of 5-methoxysalicylaldehyde was used. The product was isolated as black crystals. Yield 1.65 g, 26%. The compound is thermochromic in solution, changing from royal blue at room temperature to emerald green by −80 °C in acetone. Anal. Calcd: C, 42.94; H, 4.91; N, 9.11. Found: C, 43.24; H, 4.90; N, 9.03. Λ_c = 154.0 μmho cm^{-1} at 30 °C and 10^{-3} M in acetone.

[Fe(3-NO$_2$Salmeen)$_2$](PF$_6$)·0.5H$_2$O was prepared as above for the parent compound, except that 3.34 g (20 mmol) of the 3-nitrosalicylaldehyde was used (the ligand product precipitates out of methanol but redissolves upon addition of the $NaOCH_3$). The crude product was recrystallized twice from CH_2Cl_2/Et_2O. The final product was isolated as dark brown crystals. Yield 4.1 g, 65%. The compound is thermochromic in solution, changing from brown at room temperature to blue-green by −80 °C in acetone. Anal. Calcd: C, 36.82; H, 3.55; N, 12.88. Found: C, 36.81; H, 3.90; N, 13.20. Λ_c = 146 μmho cm^{-1} at 30 °C and 10^{-3} in acetone.

[Fe(5-NO$_2$Salmeen)$_2$](PF$_6$)·0.5H$_2$O was prepared the same as for the 3-nitrosalicylaldehyde compound except that 3.34 g (20 mmol) of the 5-nitrosalicylaldehyde was used. The product was isolated as dark brown crystals. Yield 1.3 g, 20%. The compound is thermochromic, changing from blue at room temperature to blue-green by −80 °C in acetone. Anal. Calcd: C, 36.82; H, 3.55; N, 12.88. Found: C, 36.53; H, 3.74; N, 13.17. Λ_c = 150 μmho cm^{-1} at 30 °C and 10^{-3} M in acetone.

Variable-Temperature Magnetic Susceptibility Data (T in K, χ_M'(cor) in cgsu mol^{-1} × 10^{-6}, μ_{eff} in μ_B). [Fe(Salmeen)$_2$](PF$_6$) (solid): 299.2, 14389, 5.89; 256.1, 16915, 5.91; 214.5, 19907, 5.87; 169, 24878, 5.82; 134.6, 30491, 5.75; 125.0, 33026, 5.75; 80, 53159, 5.86; 72.5, 55035, 5.65; 49.5, 79500, 5.61; 23.0, 155400, 5.35; 12.4, 272767, 5.12.

[Fe(Salmeen)$_2$](PF$_6$)(acetone): 314, 11290, 5.35; 285, 10925, 5.01; 275.5, 10867, 4.91; 268, 9895, 4.62; 258, 8991, 4.32; 246, 8550, 4.12; 237, 7737, 3.84; 226.5, 6707, 3.50; 216, 6255, 3.30; 200, 4482, 2.69; 190, 4147, 2.52.

[Fe(Salmeen)$_2$](PF$_6$) (CH$_3$CN): 315.2, 10940, 5.25; 286.1, 10650, 4.94; 270.6, 10230, 4.70; 258, 9773, 4.49; 247.3, 9122, 4.25; 239.6, 8172, 3.96.

[Fe(Salmeen)$_2$](PF$_6$) (CH$_3$OH): 315.2, 9191, 4.81; 286.1, 8507, 4.41; 270.6, 7424, 4.01; 259, 6407, 3.64; 247.3, 5527, 3.31; 239.6, 5338, 3.20.

[Fe(Salmeen)$_2$](PF$_6$) (CH$_2$Cl$_2$): 310.4, 9295, 4.80; 301.6, 9587, 4.81; 291, 9227, 4.63; 277, 8898, 4.44; 270.6, 8883, 4.38; 255.1, 7436, 3.89; 234.7, 6700, 3.55; 233.3, 6608, 3.51; 227, 6615, 3.46; 233.3, 5751, 3.16; 212.9, 4354, 2.72.

[Fe(Salmeen)$_2$](PF$_6$) (Me$_2$SO): 310.4, 8643, 4.63.

[Fe(3-OCH$_3$Salmeen)$_2$](PF$_6$) (solid): 297.8, 4254, 3.20; 259.7, 3569, 2.73; 229.5, 3619, 2.59; 202.8, 3936, 2.54; 170.5, 4538, 2.50; 125.2, 5426, 2.34; 104.5, 6163, 2.28; 78.2, 8506, 2.32.

[Fe(3-OCH$_3$Salmeen)$_2$](PF$_6$) (acetone): 314, 12350, 5.59; 285, 12217, 5.30; 275.5, 12192, 5.20; 272, 12212, 5.18; 268.5, 11605, 5.01; 261.5, 12202, 5.07; 246, 12340, 4.95; 235.5, 11442, 4.66; 235.5, 12100, 4.79; 226, 11380, 4.55; 221.5, 11450, 4.52; 221, 11590, 4.54; 216, 11100, 4.40; 209, 10344, 4.18; 196, 8445, 3.65; 182.6, 8032, 3.43.

[Fe(4-OCH$_3$Salmeen)$_2$](PF$_6$) (solid): 298.4, 13800, 5.76; 297, 13800, 5.75; 266, 15259, 5.72; 162, 20204, 5.13; 138, 21362, 4.88; 113, 25263, 4.80; 108.7, 25879, 4.76; 89.8, 30727, 4.70; 70.2, 36672, 4.54; 40.0, 63200, 4.50; 18.0, 132711, 4.37.

[Fe(4-OCH$_3$Salmeen)$_2$](PF$_6$) (acetone): 314.3, 10920, 5.24; 293.9, 10960, 5.07; 283.2, 11200, 5.04; 265.8, 11580, 4.96; 254.1, 11690, 4.87; 245.4, 11810, 4.81; 230.8, 11970, 4.70; 221.1, 12090, 4.62; 209.5, 10850, 4.26; 190.1, 9373, 3.77.

[Fe(5-OCH$_3$Salmeen)$_2$](PF$_6$) (solid): 295.4, 13888, 5.75; 263.2, 15017, 5.65; 217.7, 16900, 5.45; 187.3, 17967, 5.21; 157.3, 18634, 4.86; 138.9, 18727, 4.58; 107.1, 18878, 4.03; 79.8, 19319, 3.52; 61.1, 19592, 3.11; 38.6, 23788, 2.72; 28.0, 30212, 2.61.

[Fe(5-OCH$_3$Salmeen)$_2$](PF$_6$) (acetone): 314, 11583, 5.41; 285, 10644, 4.95; 275.5, 10291, 4.78; 272, 10244, 4.74; 268.5, 9797, 4.61; 261.5, 9153, 4.39; 246, 7787, 3.93; 235.5, 6933, 3.62; 226, 6182, 3.36; 221.5, 5954, 3.26; 221, 5910, 3.25; 216, 5502, 3.10; 209, 4924, 2.88; 196, 4129, 2.55; 182.6, 3873, 2.39.

[Fe(3-NO$_2$Salmeen)$_2$](PF$_6$)·0.5H$_2$O (solid): 298.5, 4756, 3.38; 269.3, 3488, 2.75; 247.4, 3641, 2.69; 220.6, 4079, 2.69; 168.3, 4661, 2.52; 137, 5351, 2.43; 103, 6840, 2.38; 78.6, 7219, 2.14.

[Fe(3-NO$_2$Salmeen)$_2$](PF$_6$)·0.5H$_2$O (CH$_3$CN): 301.6, 6288, 3.89; 291, 5409, 3.55; 272.5, 4908, 3.27; 269.6, 4828, 3.23; 257, 4571, 3.06; 240.5, 3960, 2.76; 232.3, 3647, 2.60.

[Fe(5-NO$_2$Salmeen)$_2$](PF$_6$)·0.5H$_2$O (solid): 294.5, 2795, 2.58; 253.5, 2610, 2.31; 189, 3017, 2.14; 112.3, 4361, 1.99; 78.6, 6086, 1.96.

[Fe(5-NO$_2$Salmeen)$_2$](PF$_6$)·0.5H$_2$O (acetone): 306.5, 4758, 3.41; 285.2, 4207, 3.10; 269.6, 3959, 2.92; 253.1, 3016, 2.47; 237.6, 2767, 2.29; 227.2, 2810, 2.26; 213.9, 2408, 2.03; 196.4, 2601, 2.02.

Results and Discussion

Molecular and Spin-State Characterization of the Complexes as Solids. The $[Fe(X\text{-Salmeen})_2]^+$ complexes of Figure 1A have been prepared as PF_6^- salts for X = H, OCH_3 (3, 4, and 5), and NO_2 (3 and 5). Elemental analysis and solution conductivities, as given in the Experimental Section, characterize the complexes as PF_6^- salts of bis-tridentate species which are uni-univalent electrolytes. Infrared spectra taken as Nujol mulls are similar to those reported for the analogous $[Fe(X\text{-Sal})_2trien](PF_6)$ complexes.[5]

As solids, the observed magnetic moments near room temperature span a range of from 2.6 μ_B (X = 5-NO_2) to 5.9 μ_B (X = H), which are values typically expected for iron(III) with $S = {}^1/_2$ (with an orbital contribution[20]) and $S = {}^5/_2$ ground states, respectively. On the other hand, the 4-OCH_3 and 5-OCH_3 derivatives possess room temperature moments which are depressed (5.75 μ_B) from the fully $S = {}^5/_2$ value, while the 3-NO_2 compound has a magnetic moment too large (3.4 μ_B) to correspond to a purely $S = {}^1/_2$ ground state. This

Table I. Variable-Temperature Mössbauer Spectral Parameters for Selected $[Fe(X\text{-}Salmeen)_2](PF_6)$ Compounds

Compound	T, K	μ_{eff}, μ_B	δ,[a,b] mm s^{-1}	Γ,[c] mm s^{-1}	ΔE_Q,[b,d] mm s^{-1}
$[Fe(Salmeen)_2](PF_6)$	296	5.89	0.49 (0.03) (hs singlet)	0.78 (0.08)[e]	
$[Fe(5\text{-}OCH_3Salmeen)_2](PF_6)$	296	5.75	0.64 (0.03) (hs doublet)	0.34 (0.03)	0.52 (0.02)
$[Fe(5\text{-}OCH_3Salmeen)_2](PF_6)$	123	4.25	0.61 (0.03) (hs singlet)	0.71 (0.08)[e]	
			0.54 (0.01) (ls doublet)	0.32 (0.02)	2.96 (0.01)
$[Fe(3\text{-}OCH_3Salmeen)_2](PF_6)$	298	3.20	0.42 (0.02) (ls doublet)	0.70 (0.04)	2.58 (0.02)

[a] Isomer shift relative to midpoint of room temperature sodium nitroprusside (SNP) spectrum. [b] Standard deviations in parentheses. [c] Half-width at half-heights (hwhh) in mm s^{-1} for the absorption peak(s). [d] Quadrupole splitting parameter. [e] Judging from the $[Fe(5\text{-}OCH_3Salmeen)_2](PF_6)$ (296 K) spectrum where $\Gamma = 0.34$ mm s^{-1} for each of two *resolved* hs quadrupole split peaks, these hs signals with $\Gamma \geq 70$ mm s^{-1} are actually probably *unresolved* doublets also.

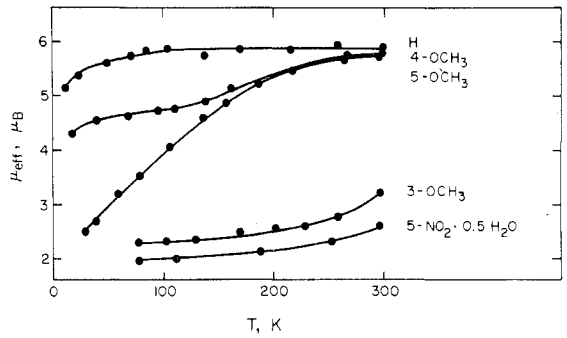

Figure 2. μ_{eff} vs. temperature data for the $[Fe(X\text{-}Salmeen)_2](PF_6)$ compounds in the solid state (the 3-NO_2 data have been omitted for clarity).

anomalous magnetic behavior can be interpreted by examining the variable-temperature susceptibility data given in the Experimental Section and shown graphically in Figure 2 as μ_{eff} vs. T plots. As seen from the plot, the X = H compound appears as a normal $S = {}^5/_2$ Curie compound from 100 to 300 K, with the moment eventually dropping off to 5.1 μ_B by 12 K. In the absence of other information, this behavior could simply be a result of a high-spin iron(III) center displaying zero field splitting. The X = 4- and 5-OCH_3 compounds appear more anomalous, with the 5-OCH_3 derivative essentially spanning the entire $S = {}^5/_2$ (5.8 μ at 295 K) to $S = {}^1/_2$ (2.6 μ_B at 28 K) spin-state range while moments for the 4-OCH_3 derivative drop from near a $S = {}^5/_2$ value (5.8 μ_B at 298 K) and tend to "plateau" in the 4.0–5.0 μ_B range at lower temperatures. In contrast, the 3-OCH_3 and 5-NO_2 derivatives are nearly $S = {}^1/_2$ compounds ($\leq$3.0 μ_B) at room temperature and gradually approach the limiting 1s value as the temperature is lowered. Data for the 3-NO_2 compound, not shown in the figure for purposes of clarity, closely resemble that for the 3-OCH_3 derivative. While most of these variable-temperature patterns could result from *inter*molecular antiferromagnetic interactions between $S = {}^5/_2$ centers, this possibility is considered unlikely, since (1) the μ_{eff} vs. T plots are field independent as measured at 3.0 and 8.5 kG, (2) the same general pattern of decreasing μ_{eff} vs. T plots are obtained in solution (as shown in Figure 4) where *inter*molecular interactions can be assumed to be negligible, and (3) variable-temperature Mössbauer spectroscopic data are inconsistent with this interpretation, as discussed below. Rather, it is more reasonable to ascribe these anomalous variable-temperature magnetic data for the $[Fe(X\text{-}Salmeen)_2]^+$ complexes to thermally dependent $(S = {}^1/_2) \rightleftarrows (S = {}^5/_2)$ spin-equilibrium processes similar to those that exist for the structurally similar and well-characterized hexadentate ligated complexes, $[Fe(X\text{-}Sal)_2trien]$ and $[Fe(AcacX)_2trien)]^+$.[5,6] At the lowest temperatures investigated ($\sim$10 K), all of the $(S = {}^1/_2) \rightleftarrows (S = {}^5/_2)$ $[Fe(X\text{-}Salmeen)_2]^+$ compounds, with the exception of the 4-OCH_3 derivative, tend to approach a lower limit value of $\sim$2.0 μ_B as expected for an $S = {}^1/_2$ state, and in no case is there any evidence for ferromagnetic impurities in the compounds which would be expected to produce an abrupt increase in the susceptibility around the Curie temperature. Such impurities have sometimes been reported to be a problem by other workers in the spin-equilibrium area.[21] As mentioned above, the 4-OCH_3 derivative has a low-temperature moment which levels between 4.0 and 5.0 μ_B and does not approach the theoretical $S = {}^1/_2$ value. For the present, this behavior is probably best attributed to unknown solid-state effects, because it does not exist in solution, as is discussed below. A consideration of the influence of the salicylaldimine ligand substituents (H, OCH_3, NO_2) on the spin-equilibria is also deferred to the solution section discussion, since it is well documented that counterion, hydration, and lattice effects can be of overwhelming importance in the solid state[22] and are likely to mask expectedly more subtle ligand substituent effects.

Thus, the $[Fe(X\text{-}Salmeen)_2]^+$ series joins a rather select group of synthetic six-coordinate iron(III) complexes which also exhibit the unusual $(S = {}^1/_2) \rightleftarrows (S = {}^5/_2)$ spin-equilibrium phenomenon as solids: the tris(dithiocarbamato)iron(III) compounds,[23] the tris(monothiocarbamato)iron(III) complexes,[7a,24,25] the tris(diselenocarbamato)iron(III) compounds,[26] the tris(monothio-β-diketonato)iron(III) complexes,[27a,b] and the aforementioned $[Fe(X\text{-}Sal)_2trien]^+$ and $[Fe(AcacX)_2trien]^+$ compounds. The $[Fe(X\text{-}Salmeen)_2]^+$ complexes are, however, the first bis-tridentate species found to exhibit the property. Furthermore, it should also be noted that while most of these $(S = {}^1/_2) \rightleftarrows (S = {}^5/_2)$ systems contain Fe–S or Fe–Se bonds where large reduction in the Racah interelectronic repulsion parameters apparently produce strong enough ligand fields to induce spin-crossover for iron(III),[28] the present $[Fe(X\text{-}Salmeen)_2]^+$ series and their hexadentate analogues have only Fe–N and Fe–O bonds. For these compounds it is probably the large tetragonal distortion from octahedral symmetry that is mainly responsible for inducing spin-crossover through extensive term state splitting of the low-spin ^2T state ($^2T \rightarrow {}^2A + {}^2E$, with further splitting of the ^2E).[29] The structural magnitude of this molecular distortion has recently been characterized by x-ray analysis of the $S = {}^1/_2$ compounds, $[Fe(Sal)_2trien]NO_3 \cdot H_2O$ and $[Fe(Sal)_2trien]Cl \cdot 2H_2O$,[16] where the ⟨Fe–ligand⟩ bond distances are found to be: Fe–N(H), 2.00 Å; Fe–N(imine), 1.93 Å; and Fe–O, 1.89 Å. It is probable that the $[Fe(X\text{-}Salmeen)_2]^+$ compounds, whose structures are presently under investigation,[30] will exhibit a similar distortion pattern.

Mössbauer spectra for several of the new $[Fe(X\text{-}Salmeen)_2](PF_6)$ complexes have also been obtained to further characterize their electronic structure and to establish an *upper* limit for the $(S = {}^1/_2) \rightleftarrows (S = {}^5/_2)$ intersystem crossing rates in the solid state. Typically fit computerized spectra are shown in Figure 3, with isomer shift (δ) and quadrupole splitting

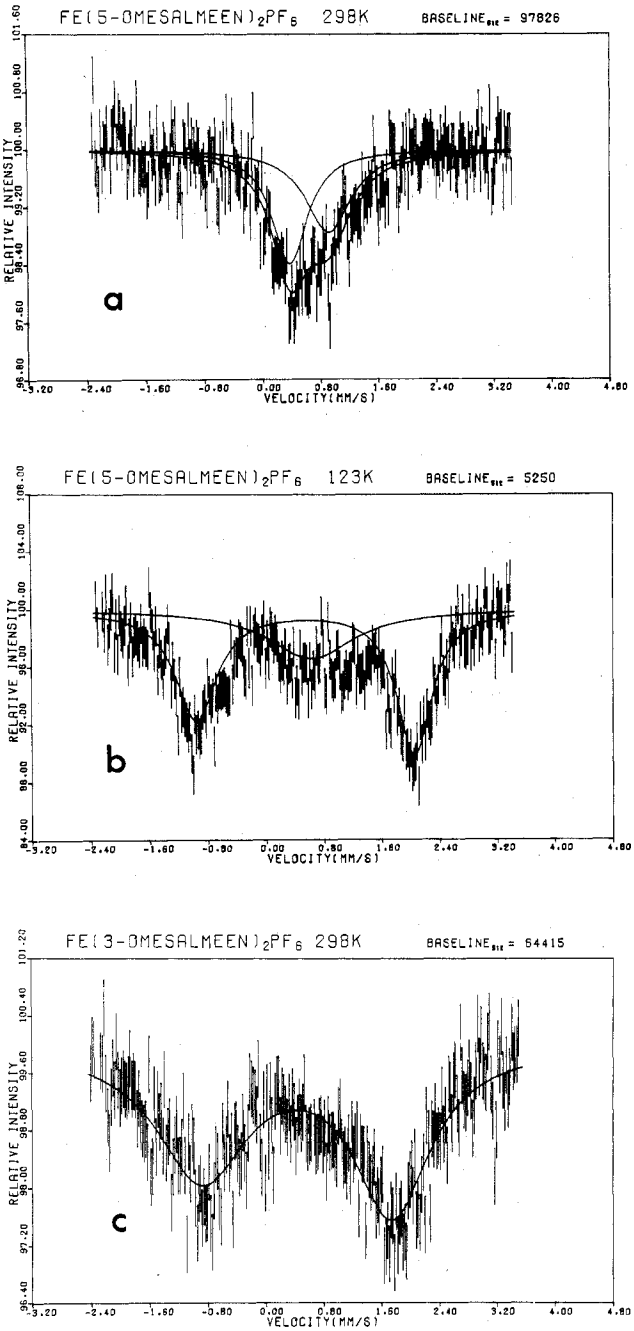

Figure 3. Mössbauer spectra of (a) [Fe(5-OCH$_3$Salmeen)$_2$](PF$_6$) at 296 K, (b) [Fe(5-OCH$_3$Salmeen)$_2$](PF$_6$) at 123 K, and (c) [Fe(3-OCH$_3$Salmeen)$_2$](PF$_6$) at 298 K.

(ΔE_Q) parameters given in Table I. For temperatures corresponding to magnetic moments of ≥ 5.7 μ_B, or that of an essentially hs $S = {}^5/_2$ state, the Mössbauer spectrum is characterized by either a broad singlet or unresolved doublet (for X = H at 296 K) or a resolved small quadrupole split doublet (for X = 5-OCH$_3$ at 296 K) with δ ranging from 0.50 to 0.65 mm s^{-1}. The resolved doublet for the X = 5-OCH$_3$ compound is shown in Figure 3a. The range of δ values for the $S = {}^5/_2$ state in these [Fe(X-Salmeen)$_2$]$^+$ complexes compares favorably to those already reported[5,6,16] for the hs form of the [Fe(X-Sal)$_2$trien]$^+$ and [Fe(AcacX)$_2$trien]$^+$ compounds, although no obvious quadrupole splitting is apparent in the latter two cases. This result could be interpreted to imply that the N_4O_2 donor atom set in the bis-tridentate [Fe(X-Salmeen)$_2$]$^+$ complexes is somehow "more distorted" than in the hexadentate species, although this is not necessarily

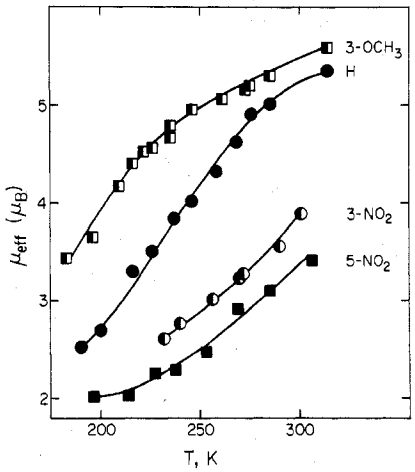

Figure 4. μ_{eff} vs. temperature data for the [Fe(X-Salmeen)$_2$](PF$_6$) compounds in acetone (the 4- and 5-OCH$_3$ data have been omitted for clarity and the 3-NO$_2$ data are for CH$_3$CN for solubility reasons).

the case, since even highly symmetrical FeO$_6$ cores in tris(acetylacetonato)iron(III) complexes are known to produce quadrupole splittings as large as 0.75 mm s^{-1}.[31] However, unlike for the [Fe(acac)$_3$] complexes, the [Fe(X-Salmeen)$_2$]$^+$ spectra do not appear to show extensive relaxation broadening[32] of the $S = {}^5/_2$ signal as the temperature is lowered. For temperatures which produce a large mole fraction of the $S = {}^1/_2$ state, the Mössbauer spectrum consists of a rather large quadrupole split doublet as shown in Figure 3c for X = 3-OCH$_3$ at 298 K where the ls state is ~70% populated. For a low-spin ^{2}T spin state an increase in ΔE_Q is to be expected, especially in the case of such highly unsymmetrical chelates as these, and the values in Table I fall in the same range of 2.0–3.0 mm s^{-1} as found for the $S = {}^1/_2$ [Fe(X-Sal)$_2$trien]$^+$ and [Fe(AcacS)$_2$trien]$^+$ cation forms. Most significant of all, however, is the Mössbauer spectrum of the 5-OCH$_3$ compound at 123 K, as shown in Figure 3b. At this temperature the magnetic moment of 4.25 μ_B corresponds to a substantial population of both spin states (60% $S = {}^1/_2$, 40% $S = {}^5/_2$) and, indeed, the spectrum consists of a superimposition of both the ls and hs signals. In no case is any evidence of signal broadening or magnetic hyperfine splitting observed which would be expected to accompany *anti*ferromagnetic interactions[33] if, indeed, such interactions contributed significantly to the anomalous μ_{eff} vs. T patterns of Figure 2. These Mössbauer results, where separate $S = {}^1/_2$ and $S = {}^5/_2$ spin signals are clearly resolved at intermediate magnetic moments, firmly establish an *upper* limit of 10^7 s^{-1} (the Mössbauer transition time scale[34]) for the ($S = {}^1/_2$) $\rightleftarrows$ ($S = {}^5/_2$) intersystem crossing rates in the *solid* state. Viewed alternatively, τ(ls) and τ(hs) are $\gtrsim$100 ns. In itself, this observation is not particularly surprising, since Mössbauer spectroscopy has established the same result for most other iron(II) and iron(III) spin-equilibrium systems, except perhaps for those associated with the tris(dithiocarbamato)- and tris(monothiocarbamato)iron(III) species.[7a,23] It is, however, significant that such data for the *solid* state, when viewed against complementary *solution*-state measurements can, in favorable instances, be used to demonstrate differing intersystem crossing rates (or spin lifetimes) in the two environments. Such is apparently the case for the present [Fe(X-Salmeen)$_2$]$^+$ complexes (vide infra).

Spin-State Properties of the Complexes in Solution. Variable-temperature magnetic susceptibility data in acetone for the [Fe(X-Salmeen)$_2$](PF$_6$) complexes are shown in Figure 4. Data shown in the figure are documented in the Experimental Section. The non-Curie behavior of all the μ_{eff} vs. T plots is consistent with the preservation of the *intra*molecular

($S = {}^1/_2$) $\rightleftarrows$ ($S = {}^5/_2$) equilibrium processes in the solution state. Furthermore, all of the curves are characteristically smooth and noticeably lacking of unpredictable solid-state patterns, such as the "plateau effect" displayed by the 4-OCH_3 compound. For this reason, solution-state data seem more satisfactory when considering ligand substituent effects and other properties which are associated with *dynamic* intersystem crossing processes.

Assuming values of 5.9 and 2.0 μ_B as the limiting hs and ls moments, the percent hs isomer for the $[Fe(X\text{-}Salmeen)_2]^+$ series in acetone decreases according to the salicylaldimine ring substituent series 3-OCH_3 (88% at 314 K) > 5-OCH_3 (82% at 314 K) > H (80% at 314 K) > 3-NO_2 (36% at 299 K) > 5-NO_2 (19% at 285 K). Furthermore, the variable-temperature studies in Figure 4 confirm this to be the pattern over the entire 200–300 K temperature range. The same general substituent ordering, i.e., $OCH_3 > H > NO_2$, was also observed for the $[Fe(X\text{-}Sal)_2trien](PF_6)$ complexes, although the analogous $[Fe(X\text{-}Salmeen)_2](PF_6)$ derivatives tend to exhibit slightly higher magnetic moments for identical substituent/temperature/solvent conditions. This implies that $10Dq_{[(X\text{-}Sal)_2trien]} > 10Dq_{[(X\text{-}Salmeen)_2]}$ for the ligand sets toward iron(III). In addition, it should be noted from the solution magnetic data that the magnitude of $10Dq$ increases according to $X = OCH_3 < H < NO_2$ for both the $[(X\text{-}Sal)_2trien]$ and $[(X\text{-}Salmeen)_2]$ series and that this dependency has been rationalized in terms of an iron(III) $\rightarrow$ ligand (π) bonding scheme for the former compounds.[5] Using the solid-state data of Figure 2, no systematic influence of ligand substituent on the position of the ($S = {}^1/_2$) $\rightleftarrows$ ($S = {}^5/_2$) equilibrium is apparent, again emphasizing the limitations of using solid data to consider such effects.

The influence of five solvents on the spin-equilibrium for the $[Fe(Salmeen)_2]^+$ parent complex has also been investigated, and the data are given in the Experimental Section. In general, acetone favors the hs state most (80% hs at 314 K) and Me_2SO the least (56% hs at 310 K) with the entire solvent series being acetone > CH_3CN > CH_3OH > CH_2Cl_2 > Me_2SO. This solvent ordering is somewhat different from that found for the $[Fe(Sal)_2trien]^+$ compound and, unlike for the $[Fe(Sal)_2trien]^+$ complex,[5] there is no obvious correlation between the observed magnetic moment and the strength of the [solvent···HN] hydrogen bonding interaction as judged by the position of $\nu_{N-H}(st)$ in the $[Fe(Salmeen)_2]^+$ infrared spectrum: acetone (3270 cm^{-1}), CH_3CN (3270 cm^{-1}), CH_3OH (3260 cm^{-1}), CH_2Cl_2 (3300 cm^{-1}). It is apparent, however, from Figure 1 that stereochemically the $[Fe(Sal)_2trien]^+$ complex (B) contains only a single type of N–H proton, while the $[Fe(Salmeen)_2]^+$ cation (A) possesses other possible arrangements of the two N–H protons relative to one another as an additional complication to any overall [solvent···HN] interaction scheme. This may explain, at least in part, the discrepancy in the solvent dependency as observed for the two series of compounds.

Solution-state thermodynamic parameters for the ($S = {}^1/_2$) $\rightleftarrows$ ($S = {}^5/_2$) intersystem crossing, as calculated from the variable-temperature magnetic susceptibility data, are shown in Table II. The parameters have been calculated by the method in ref 5. The $\Delta H°$ and $\Delta S°$ values are all similar regardless of substituent kind or position or the solvent system. Qualitatively the major contribution to $\Delta H°$ (3–4 kcal mol^{-1}) undoubtedly reflects the changing iron(III)–(donor atom) bond distances and energies that are known to always accompany (ls) $\rightleftarrows$ (hs) spin-conversion processes. For the $[Fe(Sal)_2trien]^+$ and $[Fe(AcacX)_2trien]^+$ complexes, which exhibit similar ranges for $\Delta H°$ in solution,[5,6] the (ls) $\rightarrow$ (hs) increase in the six bond distances (Δr) averages 0.13 Å, with the four iron–nitrogen distances changing the most by 0.17 Å and the two iron–oxygen distances the least by 0.05 Å.[16] The coordination sphere reorganization energy, E_r, which accompanies the spin conversion, can be estimated using eq 1.[35,36] Assuming typical values for the sum of the hs and ls force constants, ($K_{hs} + K_{ls}$), in the range of 1.5×10^5–2.0×10^5 dyn cm^{-1} and $r = 0.13$ Å for the present case, E_r is calculated to be 2.7–3.7 kcal mol^{-1}. This range is in good agreement with the $\Delta H°$ values in Table II, suggesting that inner-sphere reorganization is, indeed, the dominant enthalpic term in the spin-equilibrium process. The $\Delta S°$ values reported in Table II contain an "electronic entropy change" of $R \ln (6/6) = 0$ expected for the $^2T \rightarrow {}^6A$ process. In reality, this change in electronic entropy is probably larger for these tetragonally distorted $[Fe(Sal)_2trien]^+$ and $[Fe(Salmeen)_2]^+$ complexes, i.e., $^2T(O_h) \rightarrow {}^2E + {}^2A$, and the spin conversions are, therefore, actually $^2E(ls) \rightarrow {}^6A(hs)$ ($R \ln (6/4) = 0.80$ eu) or $^2A(ls) \rightarrow {}^6A(hs)$ ($R \ln (6/2) = 2.18$ eu) cases. The remaining, and therefore major, contribution to $\Delta S°$ probably arises from solvation sphere reorganization that accompanies the (ls) $\rightarrow$ (hs) conversion. Thus, some solvent dependency on $\Delta S°$, as observed for the parent compound, should be expected.

$$E_r = 6\left[\frac{K_{hs} + K_{ls}}{2}\right]\left[\frac{\Delta r}{2}\right]^2 \quad (1)$$

Measurement and Interpretation of the ($S = {}^1/_2$) $\rightleftarrows$ ($S = {}^5/_2$) Intersystem Crossing Rates. The variable-temperature

Table II. Thermodynamic Parameters for the $[Fe(X\text{-}Salmeen)_2]^+$ (ls) $\rightarrow$ (hs) Processes in Solution

Compound	Solvent	$\Delta H°$,[a,b] kcal/mol	$\Delta S°$,[a,b] eu
Parent (X = H)	Acetone	3.76 ± 0.05	14.59 ± 0.21
	CH_3CN	3.16 ± 0.10	12.34 ± 0.36
	CH_3OH	3.85 ± 0.18	13.27 ± 0.65
	CH_2Cl_2	2.83 ± 0.11	10.20 ± 0.40
3-OCH_3	Acetone	2.34 ± 0.04	10.65 ± 0.15
4-OCH_3	Acetone	1.54 ± 0.10	7.12 ± 0.42
5-OCH_3	Acetone	4.01 ± 0.07	15.45 ± 0.23
3-NO_2	CH_3CN	3.29 ± 0.16	9.58 ± 0.61
5-NO_2	Acetone	5.46 ± 0.55	16.17 ± 2.19

[a] Determined from magnetic susceptibility data (with standard deviation) assuming $K_{eq} = [hs]/[ls]$ and $\mu_{eff}(hs) = 5.9\ \mu_B$ and $\mu_{eff}(ls) = 2.0\ \mu_B$. [b] Calculated as described in ref 5.

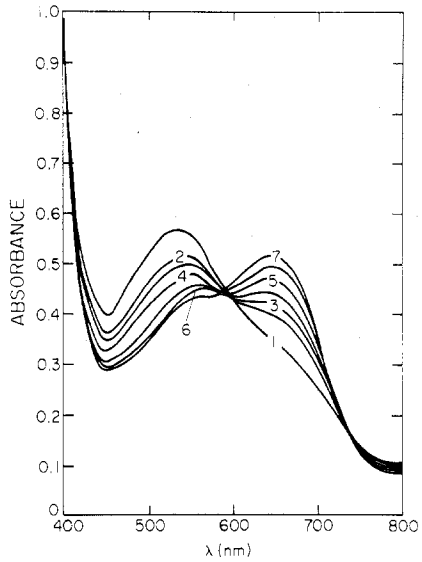

Figure 5. Variable-temperature electronic spectrum of $[Fe(Salmeen)_2](PF_6)$ in methanol at (1) 295 K, (2) 266 K, (3) 258 K, (4) 247 K, (5) 235 K, (6) 226 K, and (7) 218 K. [Fe] $\sim 10^{-3}$ M.

Table III. Electronic Spectral Data for [Fe(Salmeen)$_2$]$^+$ and [Fe(X-Salmeen)$_2$]$^+$ Complexes

A. Variable-Temperature Electronic Spectral Data for the [Fe(Salmeen)$_2$]$^+$ Complex in Methanol

Temp, K	ϵ(ls band) at 15 500 cm^{-1}	ϵ(hs band) at 18 870 cm^{-1}
295	1160	2350
266	1440	2110
258	1550	2030
247	1710	1900
235	1860	1760
226	1980	1680
218	2080	1620

B. Electronic Spectral Data for the [Fe(X-Salmeen)$_2$]$^+$ Complexes in Methanol at Room Temperature

Compound	λ_{max}, cm^{-1}	ϵ_{max}
Parent (X = H)	28 570	>10 000
	18 870 (hs)	2 350
	15 500 (ls)	1 160
3-OCH$_3$	18 180 (hs)	1 160
4-OCH$_3$	28 570	>10 000
	21 980	2 850
	18 940 (hs)	3 030
5-OCH$_3$	26 310	7 590
	21 050	1 740
	17 040 (hs)	2 160
3-NO$_2$	27 780	>10 000
	19 230 (hs)	1 820
	16 450 (ls)	1 250
5-NO$_2$	26 310	>10 000
	18 180 (hs)	2 270
	16 390 (ls)	2 430

electronic spectrum of [Fe(Salmeen)$_2$](PF$_6$) in methanol is shown in Figure 5. In general, the spectrum is characterized in the visible by a low-energy CT band centered at 660 nm (15 500 cm^{-1}) which increases in intensity with decreasing temperature and a higher energy band at 530 nm (18 870 cm^{-1}) which decreases in intensity with decreasing temperature. Band position and intensity data for the figure are given in Table III(A). Because of this temperature-dependent spectral pattern and the magnetic susceptibility data (vide supra), the lower energy band is assigned to the $S = {}^1/_2$ state and the higher energy band to the $S = {}^5/_2$ spin state. The strong temperature dependency of the [Fe(Salmeen)$_2$]$^+$ spectrum is typical of the entire series of complexes and explains their striking thermochromicity in solution. Typical thermochromic properties for each compound are given in the Experimental Section and room temperature electronic spectral parameters characterizing the PF$_6^-$ salts in methanol for all the derivatives are shown in Table III(B), along with the $S = {}^1/_2$ and $S = {}^5/_2$ band assignments. The presence of separate ls and hs spectral bands is consistent with an $(S = {}^1/_2) \rightleftarrows (S = {}^5/_2)$ intersystem crossing process which is *slow* on the electronic transition time scale, e.g., spin-conversion rates of $<10^{15}$ s^{-1} with τ(spin state) $> 10^{-15}$ s.

To measure directly the forward and reverse intersystem crossing rate constants, k_1 and k_{-1}, for the [Fe(X-Salmeen)$_2$]$^+$

$$(S = {}^1/_2) \underset{k_{-1}}{\overset{k_1}{\rightleftarrows}} (S = {}^5/_2) \qquad (2)$$

intersystem crossings, laser stimulated Raman temperature-jump kinetics has been employed. The instrumentation[12] and experimental methods[13,15,36] have been previously described; however, a few explanatory comments are given here. The 1.06 μ radiation from a Q-switched Nd-glass laser (20 J/25 ns pulse) is Raman shifted to 1.41 μ (2 J/25 ns pulse) in liquid N$_2$. Water and alcohols absorb at 1.41 μ and these solvents can be directly heated by this technique. In the present studies, an acetone/CH$_3$OH solvent mixture (1:5 by volume) has been employed as effective compromise between solubility requirements and efficient sample heating. The temperature-jump (1–5°) produces changes in the CT electronic absorption spectrum associated with changes in the temperature-dependent populations of the two spin states. These absorbance changes are monitored (either the hs or ls band) using a xenon lamp–monochromator–photomultiplier system. The experimentally observed relaxation traces are displayed on an oscilloscope and photographed. The first-order relaxation time constants, τ in ns, are then determined by one of two methods, depending on the approximate relaxation time (τ) range: (1) If $\tau > 30$ ns, the usual log $(I_\infty - I)$ vs. time plots are used[37] where I is the intensity of the light passing through the solution at time, t, and I_∞ is the limiting value of the intensity at long times. For the small intensity changes measured in these experiments, this amounts to plotting the log of the absorbance or concentration changes. (2) If $\tau \lesssim 30$ ns, the "second method of moments" integral deconvolution procedure must be employed.[38,39] This approach becomes necessary when $\tau \lesssim 30$ ns because the duration of the laser pulse (~25 ns) sets a lower limit for measurable optical changes. Details of this data treatment method for obtaining spin lifetimes are given elsewhere.[15]

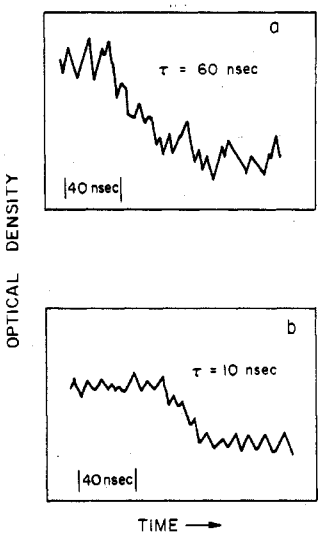

Figure 6. Laser Raman temperature-jump relaxation trace for (a) [Fe(Sal)$_2$trien]$^+$ with τ(+4 °C) = 60 ns (ref 5) and (b) [Fe(Salmeen)$_2$]$^+$ in 1:5 acetone/methanol solution with τ(−3 °C) = 10 ns as monitored at 530 nm (18 870 cm^{-1}); [Fe] = 2.5×10^{-3} M.

The equilibrium constants for the (ls) $\rightleftarrows$ (hs) processes (K_{eq} = [hs]/[ls]) were obtained from solution magnetic susceptibility data using the NMR method of Evans.[17,18] Rate constants, k_1 and k_{-1}, and the lifetimes of the spin states, τ(ls) = $(k_1)^{-1}$ and τ(hs) = $(k_{-1})^{-1}$, were calculated from the measured values of K_{eq} and τ by solving eq 3 and 4 simultaneously. First-order relaxation times are reported as the average of at least six determinations. The equilibrium constants are, of course, temperature dependent and have been determined independently for each compound and set of conditions used. The electronic spectrum of the sample was recorded before and after the T-jump experiment to check for compound decomposition; in all cases it was found to be unchanged.

$$K_{eq} = k_1/k_{-1} \qquad (3)$$

$$\tau^{-1} = k_1 + k_{-1} = [\tau(\text{ls})]^{-1} + [\tau(\text{hs})]^{-1} \qquad (4)$$

Figure 6a shows a typical spin-relaxation trace for [Fe(Sal)$_2$trien](PF$_6$) (~10^{-3} M) in methanol at +4 °C, where τ has been determined to be 60 ns.[5] The maximum error in this value is estimated at ±15 ns, based on the range of values

Table IV. Relaxation Times and

$$\text{(Low-Spin)} \underset{k_{-1}}{\overset{k_1}{\rightleftharpoons}} \text{(High-Spin)}$$

Intersystem Crossing Rate Constants for the $[Fe(X\text{-Salmeen})_2]^+$ Complexes[a]

Compound	Initial, temp, °C	K_{eq}[b]	τ,[c] ns	k_1, s^{-1} [τ(ls),[d] ns]	k_{-1}, s^{-1} [τ(hs),[d] ns]
Parent (X = H)	20	1.31	9	7.1×10^7 [14]	5.4×10^7 [18]
	−3	0.75	10	4.8×10^7 [21]	6.4×10^7 [16]
3-OCH_3	25	2.79	8	9.2×10^7 [11]	3.3×10^7 [30]
	−1	1.71	10	6.3×10^7 [16]	3.7×10^7 [27]
4-OCH_3	19	1.67	11	5.7×10^7 [18]	3.4×10^7 [29]
	−8	1.33	10	5.7×10^7 [18]	4.3×10^7 [23]
5-OCH_3	−7	0.72	9	4.6×10^7 [22]	6.4×10^7 [15]
3-NO_2	21	0.34	8	3.2×10^7 [32]	9.3×10^7 [11]
	−4	0.18	5	3.1×10^7 [33]	1.7×10^8 [6]
5-NO_2	22	0.18	7	2.2×10^7 [46]	1.2×10^8 [8]
	−5	0.10	5	1.8×10^7 [55]	1.8×10^8 [6]

[a] All data determined in acetone/methanol solution, 1:5 by volume. [b] Equilibrium constant defined as K_{eq} = [hs]/[ls] and determined from the experimentally measured magnetic moment, assuming μ_{eff}(hs) = 5.9 μ_B and μ_{eff}(ls) = 2.0 μ_B. [c] Relaxation time in ns obtained by the "second method of moments" deconvolution approach of the raw data as described in ref 15. Determined from an average of at least six oscilloscope traces. Maximum estimated error is ±10 ns. [d] Spin state lifetime: τ(spin state) = k^{-1}.

obtained from six different lasing experiments on the same sample. With K_{eq} = 0.89, $k_1 = 8.3 \times 10^6$ s^{-1} [τ(ls) = 120 ns] and $k_{-1} = 9.1 \times 10^6$ s^{-1} [τ(hs) = 110 ns] for the $[Fe(Sal)_2trien]^+$ complex under these conditions. In comparison, the relaxation trace for the $[Fe(Salmeen)_2]^+$ cation in acetone/CH_3OH at −3 °C is shown in Figure 6b, where τ is found to be $\simeq$ 10 ns. The relaxation trace in 6b was measured monitoring the $S = {}^5/_2$ band wavelength (530 nm, 18 870 cm^{-1}) and the same result is obtained if the $S = {}^1/_2$ band (660 nm, 18 870 cm^{-1}) is monitored, except that a trace is observed in which the optical density *increases* with time. At the isosbestic point (580 nm) no trace is observed. These facts are strong evidence that the absorbance changes observed in the *T*-jump experiment are, indeed, due to changes in the spin-state populations. The trace in 6b is less noisy[40] than that of 6a, and as such the error for the $[Fe(Salmeen)_2]^+$ complexes is estimated to be somewhat smaller at ±10 ns.

Calculated relaxation times and intersystem crossing rate constants for all the $[Fe(X\text{-Salmeen})_2](PF_6)$ complexes are given in Table IV. Assuming an error in the reported relaxation times of ~10 ns, the observed relaxation time constants appear independent of the X-substituent and temperature (−8 to +20 °C) and are all $\lesssim$20 ns. Due to differences in K_{eq}, rate constants for the different derivatives span a range of from 3.1×10^7 s^{-1} [τ(ls) = 33 ns] to 1.8×10^8 s^{-1} [τ(hs) = 6 ns]. Several conclusions can be drawn from these results. Firstly, the intersystem crossing rates for the $[Fe(X\text{-Salmeen})_2]^+$ complexes in *solution* appear to be *faster* than in the *solid* state, as judged from the above Mössbauer results.[34] Exactly how much faster cannot be determined unless methods are developed for directly measuring spin-conversion rates in solids. Secondly, the lack of a measurable temperature dependency of the rate constants indicates that $\Delta H^\circ \approx \Delta H^\ddagger$ for these intersystem crossings. In fact, it has recently been estimated that $\Delta H^\ddagger - \Delta H^\circ \approx 1$ kcal mol^{-1} for a number of other (ls) $\rightleftarrows$ (hs) processes in solution where the spin-equilibrium phenomenon has been modeled in terms of an internal electron-transfer reaction.[36] And finally, the ($S = {}^1/_2$) $\rightleftarrows$ ($S = {}^5/_2$) intersystem crossing rates for the present bis-tridentate $[Fe(X\text{-Salmeen})_2]^+$ complexes appear *faster* than those for the electronically similar $[Fe(Sal)_2trien]^+$ hexadentate compound. It is tempting to rationalize this observation in terms of the differing molecular structure of the two species, since the "more flexible" tridentate ligand system could conceivably facilitate intersystem crossing by offering less structural restraint to the inner-coordination sphere reorganization process.[10,36]

Acknowledgment. Support of this work by the National Science Foundation, the Robert A. Welch Foundation (Grant C-627), the donors of the Petroleum Research Fund, as administered by the American Chemical Society, and NASA under Materials Grant 44-006-001 is gratefully acknowledged. E.V.D. also thanks the U.S. Energy Research and Development Administration for a summer fellowship and travel grant to Brookhaven under the auspices of the Oak Ridge Associated Universities Program; in addition, we are indebted to Dr. Norman Sutin for his generous sponsorship of the program and many enlightening discussions during the course of the work. Liquid helium for the magnetic susceptibility studies was obtained from the Helium Liquification Facility operated under Navy contract at Rice University.

Registry No. $[Fe(Salmeen)_2](PF_6)$, 65293-56-3; $[Fe(3\text{-}OCH_3Salmeen)_2](PF_6)$, 65293-76-7; $[Fe(4\text{-}OCH_3Salmeen)_2](PF_6)$, 65293-74-5; $[Fe(5\text{-}OCH_3Salmeen)_2](PF_6)$, 65293-72-3; $[Fe(3\text{-}NO_2Salmeen)_2](PF_6)$, 65293-70-1; $[Fe(5\text{-}NO_2Salmeen)_2](PF_6)$, 65293-68-7.

References and Notes

(1) Presented in part at the Southwest Regional Meeting of the American Chemical Society, Fort Worth, Texas, Dec 1976.
(2) NASA Predoctoral Fellow.
(3) U. S. Energy Research and Development Administration Predoctoral Fellow, Summer 1976, at Brookhaven National Laboratory.
(4) Robert A. Welch Foundation Predoctoral Fellow.
(5) M. F. Tweedle and L. J. Wilson, *J. Am. Chem. Soc.*, **98**, 4824 (1976).
(6) E. V. Dose, K. M. M. Murphy, and L. J. Wilson, *Inorg. Chem.*, **15**, 2622 (1976).
(7) (a) K. R. Kunze, D. L. Perry, and L. J. Wilson, *Inorg. Chem.*, **16**, 594 (1977); (b) M. F. Tweedle and L. J. Wilson, *Rev. Sci. Instrum.*, in press.
(8) M. A. Hoselton, L. J. Wilson, and R. S. Drago, *J. Am. Chem. Soc.*, **97**, 1722 (1975).
(9) L. J. Wilson, D. Georges, and M. A. Hoselton, *Inorg. Chem.*, **14**, 2968 (1975).
(10) M. A. Hoselton, R. S. Drago, L. J. Wilson, and N. Sutin, *J. Am. Chem. Soc.*, **98**, 6967 (1976).
(11) M. G. Simmons and L. J. Wilson, *Inorg. Chem.*, **16**, 126 (1977).
(12) D. H. Turner, G. W. Flynn, N. Sutin, and J. V. Beitz, *J. Am. Chem. Soc.*, **94**, 1554 (1972).
(13) J. K. Beattie, N. Sutin, D. H. Turner, and G. W. Flynn, *J. Am. Chem. Soc.*, **95**, 2052 (1973).
(14) J. K. Beattie, University of Sydney, private communication.
(15) E. V. Dose, M. F. Tweedle, L. J. Wilson, and N. Sutin, *J. Am. Chem. Soc.*, **99**, 3886 (1977).
(16) E. Sinn, G. Sim, E. V. Dose, M. F. Tweedle, and L. J. Wilson, *J. Am. Chem. Soc.*, in press.
(17) D. F. Evans, *J. Chem. Soc.*, 2003 (1959).
(18) D. Ostfeld and I. A. Cohen, *J. Chem. Educ.*, **49**, 829 (1972).
(19) B. L. Chrisman and T. A. Tumolillo, *Comput. Phys. Commun.*, **2**, 322 (2975).
(20) B. N. Figgis, *Trans. Faraday Soc.*, **57**, 204 (1961).
(21) E. Konig and S. Kremer, *Theor. Chim. Acta*, **20**, 143 (1971); **23**, 12 (1971).
(22) See, for example, H. A. Goodwin and R. N. Sylva, *Aust. J. Chem.*, **21**, 83 (1968); C. M. Harris, T. N. Lockyer, R. L. Martin, H. R. H. Patil, E. Sinn, and I. M. Stewart, *ibid.*, **22**, 2105 (1969).
(23) See, for example, G. R. Hall and D. N. Hendickson, *Inorg. Chem.*, **12**, 2269 (1973).
(24) H. Nakajima, T. Tanaka, H. Kobayashi, and I. Tsujikawa, *Inorg. Nucl. Chem. Lett.*, **12**, 689 (1976).

(25) J. Ahmed and J. A. Ibers, *Inorg. Chem.*, **16**, 935 (1977).
(26) D. De Filippo, P. Deplano, A. Diaz, and E. F. Trogu, *Inorg. Chim. Acta*, **17**, 139 (1976).
(27) (a) M. Cox, J. Darken, B. W. Fitzsimmons, A. W. Smith, L. F. Larkworthy, and K. A. Rogers, *J. Chem. Soc., Dalton Trans.*, 1191 (1972); (b) B. F. Hoskin and C. D. Panna, *Inorg. Nucl. Chem. Lett.*, **11**, 409 (1975).
(28) C. K. Jorgensen, *Adv. Chem. Phys.*, **8**, 47 (1965), and references therein.
(29) R. J. Butcher and E. Sinn, *J. Am. Chem. Soc.*, **98**, 2440, 5159 (1976).
(30) E. Sinn and L. J. Wilson, to be submitted for publication.
(31) G. M. Bancroft, A. G. Maddock, W. K. Ong, R. H. Prince, and A. J. Stone, *J. Chem. Soc. A*, 1966 (1967).
(32) R. M. Housley and H. de Waard, *Phys. Lett.*, **21**, 90 (1966).
(33) N. N. Greenwood and T. C. Gibbs, "Mössbauer Spectroscopy", Chapman and Hall, London, 1971, p 63.
(34) The characteristic time of measurement in Mössbauer spectroscopy is the mean lifetime of the excited Mössbauer level: $\tau(ex) = 1.4 \times 10^{-7}$ s (or 140 ns) in the ^{57}Fe case. If the time of spin conversion between the ls and hs spin states is comparable to the lifetime, τ(spin state) $\gtrsim \tau$(ex), two Mössbauer spectra representing both hs and ls states will be observed. On the other hand, if the spin conversion time is much shorter than the transition time, τ(spin state) $\ll \tau$(ex), an "averaged" spectrum should be observed.
(35) H. C. Stynes and J. A. Ibers, *Inorg. Chem.*, **10**, 2304 (1971).
(36) E. V. Dose, M. A. Hoselton, N. Sutin, M. F. Tweedle, and L. J. Wilson, *J. Am. Chem. Soc.*, in press.
(37) See, for example, ref 10.
(38) S. S. Brody, *Rev. Sci. Instrum.*, **28**, 1021 (1957); D. H. Cooper, *ibid.*, **37**, 1407 (1966).
(39) J. N. Demas and G. A. Crosby, *Anal. Chem.*, **42**, 1010 (1970).
(40) Fundamental limitation on the resolution obtainable in these *T*-jump experiments arises from (1) the duration of the heating pulse (~25 ns), (2) the enthalpy change ($\Delta H°$) associated with the spin transition, and (3) the differences in the molar absorptivities of the hs and ls complexes. The first limitation can be overcome using the method of moments deconvolution approach.[15] The last two limitations decrease the signal-to-noise ratio (Figure 6) but, in general, it has been found possible to optimize the detection system so that these are also not limiting factors.

Contribution from the Department of Chemistry,
William Marsh Rice University, Houston, Texas 77001

Solution-State Spin-Equilibrium Properties of the Tris[2-(2-pyridyl)imidazole]iron(II) and Tris[2-(2-pyridyl)benzimidazole]iron(II) Cations

KAREN A. REEDER,[1] ERIC V. DOSE,[2] and LON J. WILSON*

Received August 3, 1977

Contrary to previous reports, the tris[2-(2-pyridyl)imidazole]iron(II) ($[Fe((py)imH)_3]^{2+}$) and tris[2-(2-pyridyl)benzimidazole]iron(II) ($[Fe((py)bimH)_3]^{2+}$) cations have been shown to be

$$^1A(S=0) \underset{k_{-1}}{\overset{k_1}{\rightleftharpoons}} {}^5T(S=2)$$

spin-equilibrium species in *solution* by variable-temperature magnetic and electronic spectral studies. Laser Raman temperature-jump kinetics has been used to directly measure the forward ($k_1 = 1.1 \times 10^7$ s^{-1}) and reverse ($k_{-1} = 1.0 \times 10^7$ s^{-1}) intersystem crossing rate constants for the *dynamic* spin-interconversion process in $[Fe((py)imH)_3]^{2+}$. The results are compared to similar kinetic data available for other iron(II) spin-forbidden/conversion processes in bis(pyrazolylborate)iron(II) and $[Fe(6\text{-}Mepy)_n(py)_m tren]^{2+}$.

Transition-metal complexes exhibiting anomalous magnetic properties arising from a thermally dependent "spin-equilibrium" between low-spin (ls) and high-spin (hs) states have been studied extensively over the almost 50 years since the phenomenon was first discovered,[3] but such studies have been largely confined to the solid state. Work done on many such compounds, especially the $^1A(ls) \rightleftarrows {}^5T(hs)$ iron(II) complexes of 2-(2-pyridyl)imidazole, $[Fe((py)imH)_3]^{2+}$ (Figure 1), and 2-(2-pyridyl)benzimidazole, $[Fe((py)bimH)_3]^{2+}$, have been hindered by the lack of understanding to date of unpredictable lattice effects arising from various degrees of hydration/solvation, anion change, and possibly *inter*molecular metal–metal magnetic exchange interactions. In particular, studies of these two iron(II) spin-equilibrium systems have been in disagreement in many instances, most likely due to varying methods of preparation and purification which have yielded different solvates, degrees of solvation, and perhaps even different crystal forms of the same solvate.[4,5] In solution, all such generally troublesome effects are eliminated or at least minimized. With this realization, we have recently been engaged in a systematic study of spin-equilibrium phenomena in the solution phase. Furthermore, solution-phase studies provide an important advantage over those in the solid state in that rapid perturbation (*T*-jump) kinetics can be employed[6-14] to directly measure first-order rate constants k_1

$$\text{low spin} \underset{k_{-1}}{\overset{k_1}{\rightleftharpoons}} \text{high spin} \qquad (1)$$

and k_{-1} for *dynamic* spin-interconversion (intersystem crossing) processes. Such studies are of fundamental importance in understanding intersystem crossing phenomena as they relate to photochemically induced excited states[15] and for a general understanding of the role of spin-multiplicity changes on electron-transfer rates.[16]

In this work we report the solution-state spin-equilibrium properties for the $[Fe((py)imH)_3]^{2+}$ and $[Fe((py)bimH)_3]^{2+}$ cations, both of which have been found to exhibit the phenomenon in solution contrary to earlier findings.[17,18] In addition, the neutral iron(III) complex of the 2-(2-pyridyl)imidazolate anion, $Fe((py)im)_3$, has also been prepared by deprotonation of $[Fe((py)imH)_3]^{2+}$, via an $Fe((py)imH)_2Cl_2$ intermediate, and characterized as low spin in both the solution and solid states.

Experimental Section

Materials. Reagent grade $FeCl_2 \cdot 4H_2O$ was obtained commercially. Reagent grade pyridine-2-carboxaldehyde from Aldrich was freshly distilled before use. All other reagents, including the 2-(2-pyridyl)benzimidazole ligand (Aldrich) were reagent grade and were used without further purification.

Physical Measurements. Magnetic measurements in solution were performed by the Evans ^1H NMR method[19] using methanol for temperature calibration. A first-order correction for changes in solvent density and sample concentration was employed.[20] UV–vis spectra were run on a Cary 17 instrument using jacketed, insulated quartz cells; reported temperatures are ±0.5 °C and were monitored with a thermistor. Solution conductivities in acetone and methanol were obtained with a Model 31 YSI conductivity bridge. Elemental analyses were performed commerically. Mass spectra were obtained on a Finnigan Model 9500 GC/MS.

0020-1669/78/1317-1071$01.00/0